

Photometric Correction of Chang'e-4 Visible and Near-infrared Imaging Spectrometer (VNIS) Data. X. B. Qi¹, J. Zhang^{*1}, Z. C. Ling^{*1}, J. Chen¹, C. Q. Liu¹, L. Liu¹, Z. P. He², R. Xu². ¹ Shandong Key Laboratory of Optical Astronomy and Solar-Terrestrial Environment, School of Space Science and Physics, Institute of Space Sciences, Shandong University, Weihai, Shandong, 264209, China (zcling@sdu.edu.cn; zhang_jiang@sdu.edu.cn). ² Key Laboratory of Space Active Opto-Electronics Technology, Shanghai Institute of Technical Physics, Chinese Academy of Sciences, Shanghai 200083, China.

Introduction: On 3 January 2019, Chang'e-4 (CE-4) landed on the lunar farside and released the Yutu-2 rover to carry out mineralogical detections with Visible and Near-infrared Imaging Spectrometer (VNIS) [1]. The VNIS consists of a visible and near-infrared (VNIR, 450–945 nm) imaging part and a non-imaging shortwave infrared part (SWIR, 900–2395 nm). All of these measurements were performed at different illumination conditions (incidence angle (i), emission angle (e), phase angle (g)) and covered a wide range of phase angles (40–112°). Hence, to accurately invert the mineralogic composition of landing area, photometric corrections is needed to normalize the CE-4 VNIS data to a standard geometry ($i = 30^\circ$, $e = 0^\circ$, $g = 30^\circ$) and enable comparisons among CE-4 data and previous observations.

In Lin's work [2], a three-order polynomial photometric model is fitted with laboratory multi-angle measurements of lunar soil analog and applied to the photometric correction of the VNIS spectra. In this work, we attempt to derive photometric correction model based on the VNIS in situ observations and compare the results with those based on models derived from lunar soil/analog measurements.

Data

During the 10th lunar day, the VNIS made 23 observations of two targets at phase angles of 55–79° and 91–112°, respectively (Fig. 1). These datasets provide a good opportunity for photometric modeling of lunar regolith.

The VNIS 2B radiance data are calibrated into bidirectional reflectance by dividing the solar irradiance, and then normalized to a Sun-Moon distance of 1 AU.

For the VNIR images, (i , e , g) for each pixel is calculated by interpolating the values of the four corner points, and averaged over 1° phase angle bin (Fig. 2a); for the SWIR spectra, central point angles are used. (Fig. 2b).

Lommel-Seeliger model: Lunar surface reflectance can be approximated by the Lommel-seeliger Law [3, 4]:

$$r(i, e, g) = \frac{\mu_0}{\mu_0 + \mu_1} f(g) \quad (1)$$

where r is bidirectional reflectance. μ_0 and μ_1 are $\cos(i)$ and $\cos(e)$. $f(g)$ describes reflectance variation with phase angle. A third order polynomial was used in this work to model $f(g)$ [2]:

$$f(g) = p_1 g^3 + p_2 g^2 + p_3 g + p_4 \quad (2)$$

The parameter values in Eq. (2) were derived for each band using the non-linear least squares methods, then VNIS data are normalized into the standard geometry by Eq. (3):

$$r_{\text{measure}}(30^\circ, 0^\circ, 30^\circ) = \frac{r_{\text{model}}(30^\circ, 0^\circ, 30^\circ)}{r_{\text{model}}(i, e, g)} r_{\text{measure}}(i, e, g) \quad (3)$$

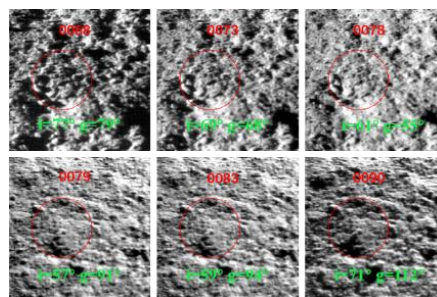


Figure 1. Representative (6 out of 23) reflectance images at 450 nm of the two detection targets measured in the tenth lunar day. The red circles and number labels indicate FOV of SWIR spectrometer and data filename released at <http://moon.bao.ac.cn/>.

Hapke model: Hapke radiative transfer model [5] was also used to compare correction results with different photometric models. The Hapke model used in this work [6, 7] is described as:

$$r(i, e, g) = \frac{\omega}{4\pi} \frac{\mu_0}{\mu_0 + \mu_1} \{ [1 + B(g)] P(g) + H(\mu_0) H(\mu_1) - 1 \} \quad (4)$$

where r is bidirectional reflectance; ω is single scattering albedo (SSA); $B(g)$ is backscattering function describing shadow-hiding opposition effect; $H(x)$ describes the multiple scattering process. $P(g)$ is the phase function and can be expressed as Legendre polynomial:

$$P(g) = 1 + b \cos(g) + c(1.5 \cos^2(g) - 0.5) \quad (5)$$

Yang et al. [2019] derived the phase function of Hapke model by using lunar analogs/samples, and $b = -$

0.20, $c = 0.16$ [7] are used in this work. Based on this model, the reflectance data at different phase angles were converted to SSA and then the REFF (reflectance factor) at standard geometry were calculated from SSA with the Eq. (4).

Results and discussion: The photometric correction results of Lommel-Seeliger model and Hapke model are compared in Fig. 3. After photometric correction, the reflectance of CE-4 regolith increases using Lommel-Seeliger model, while decreases using Hapke model. It can also be seen that for the spectrum of the same target, the spectral curves are separated after correction by using the Hapke model. This may be because the parameters b and c we used were obtained from lunar analogs, the physical properties (e.g. porosity) of lunar surface regolith and laboratory samples are different and these two parameters are essentially wavelength-dependent. As shown in Fig. 3a-c, the corrected spectra don't overlap with each other. It is probably due to the influence of surface roughness as evident from that the shadowed pixels in images increase with increasing solar incident angles and phase angles (Fig. 1).

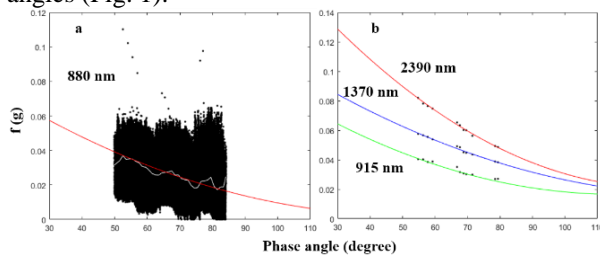


Figure 2. Examples of phase function curves for wavelengths of 880 nm, 915 nm, 1370 nm, and 2390 nm. The white line in (a) is the averaged pixel values within 1° phase angle.

Lunar soil analogs were used to test the two photometric corrections models. The analogs spectra were measured using the VNIS engineering model at 9 phase angles varying from 28° to 103° (Fig. 3d-f). The analogs were ground and sieved to grain size of 20-100 μm , and were flattened out before measurements to suppress shadowing effects caused by surface roughness. The SWIR spectra corrected with the Lommel-Seeliger model coincide well except the one measured at very large phase angle ($g > 97^\circ$), which probably caused by stray light from the illuminant. While the reflectance of VNIR corrected with the Lommel-Seeliger model deviate from each other, probably due to shadows in the VNIS images. Preliminarily, the Hapke model with constant b and c values used in this work didn't work well for certain bands, revealing the wavelength dependence of Legendre polynomial coefficients.

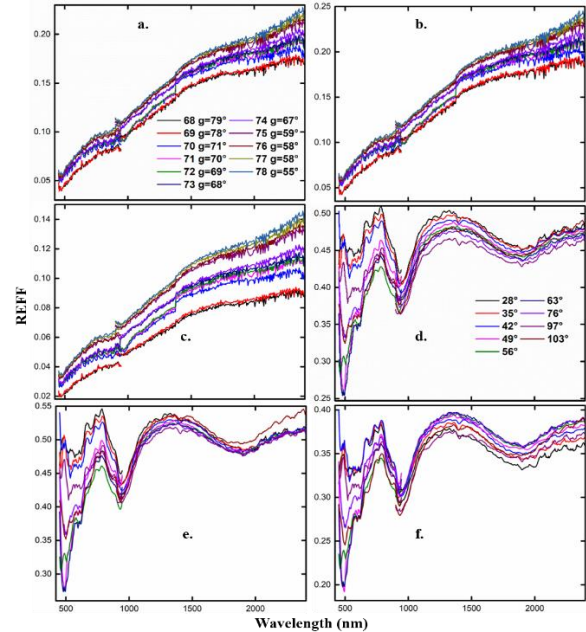


Figure 3. Comparisons of photometric correction results. a) CE-4 spectra before photometric correction. b) CE-4 spectra corrected with Lommel-Seeliger model. c) CE-4 spectra corrected with Hapke model. d) VNIS spectra of analog before photometric correction. e) analog spectra corrected with Lommel-Seeliger model. f) analog spectra corrected with Hapke model.

Conclusion:

1. Photometric modeling with analogs cannot represent the photometric characteristics of actual lunar soils (differences in physical properties, such as porosity, etc.);
2. Our empirical model obtained from the CE-4 VNIS in situ observations is not suitable for very large phase angle ($> 97^\circ$), possibly caused by stray light.

Acknowledgments: This work is supported by the National Natural Science Foundation of China (11941001, 41972322, U1931211), the Pre-research project on Civil Aerospace Technologies No. D020102 funded by China National Space Administration (CNSA), the Natural Science Foundation of Shandong Province (ZR2019MD008), Qilu (Tang) Young Scholars Program of Shandong University, Weihai (2015WHWLJH14), and Physical-Chemical Materials Analytical & Testing Center of Shandong University at Weihai.

References: [1] Wu W. et al. (2017) *J. Deep Space Exploration*, 4(2), 111-117. [2] Lin H. et al. (2019) *National Science Review*. [3] Hapke B. (1993) In *New York: Cambridge University Press*. 469. [4] Zhang J. et al. (2013) *Chinese science bulletin* 58.36, 4588-4592. [5] Hapke B. (2012) *Cambridge University Press*. [6] Sun L et al. (2019) *Lunar and Planetary Science Conference*. Vol. 50. [7] Yang Y. et al. (2019) *JGR*, 124.1, 31-60.